Published in IET Communications
Received on 8th May 2012
Revised on 25th November 2012
Accepted on 17th December 2012
doi: 10.1049/iet-com.2012.0244

ISSN 1751-8628

Low-complexity symbol timing error detection for quasi-orthogonal space–time block codes

Pawel A. Dmochowski

School of Engineering and Computer Science, Victoria University of Wellington, Wellington, New Zealand
E-mail: pdmochowski@ieee.org

Abstract: The author presents the design and analysis of low-complexity symbol timing error detectors (TEDs) for timing synchronisation in quasi-orthogonal space–time block code (QOSTBC) receivers. The estimators operate on data symbols and approximate decision variables, producing timing error measurements which are shown to be robust to channel fading. In evaluating the detector S-curve for the general form of the estimator, the author shows that the result is independent of the constellation rotation angle employed by the code. The expressions for the estimation error variance and TED signal-to-noise ratio are also obtained, with the analysis carried out under the assumptions of perfect data and channel knowledge at the receiver. Through system simulations, the effects of decision errors on the detector characteristics are examined, and the overall system performance is evaluated, where the proposed TEDs are incorporated into the receiver timing loop. Receivers with perfect channel knowledge and pilot-based channel estimation are considered. Symbol error rate results show timing synchronisation loss of less than 0.5 dB for a receiver with perfect channel information. In addition, it is shown that the receiver is able to track the timing variations two orders of magnitude faster than required by the present-day hardware oscillators.

1 Introduction

It is well known that the receiver's ability to synchronise the timing epoch is critical to the overall performance of multiple-input multiple-output (MIMO) systems [1–6]. A number of papers dealing with timing synchronisation in MIMO receivers (see e.g. [2–4]) have dealt with timing acquisition by virtue of the oversampled log-likelihood function (LLF) derived from orthogonal training sequences. In contrast to these methods, a very low-complexity approach to timing error tracking in orthogonal space–time block coding (OSTBC) receivers was presented in [7]. The authors of [7] have shown that a low-complexity function of data symbols (or decisions) and the OSTBC decision variables can be used to obtain a measurement of the symbol timing error that is robust to the channel state.

In this paper we extend the results of [7] by considering quasi-OSTBC (QOSTBC) and rotated-QOSTBC (ϕ-QOSTBC) systems. In contrast to OSTBC, where the simplified detection process provided decision variables used for timing error detector (TED) design and analysis, the detection process for QOSTBC involves the optimisation of a maximum likelihood (ML) metrics, which does not allow a similar approach. As a result, for the purpose of TED, we consider the use of approximate decision variables, derived from OSTBC detection. This enables a systematic TED design as well as S-curve and estimation error variance analysis for QOSTBC. Similar to [7], the analysis assumes correct data decisions and perfect channel knowledge at the receiver. The effects of decision errors and channel estimation errors do not allow for analytical tractability and thus these are evaluated via system simulations.

The contributions of this paper are as follows:

- By considering approximate decision variables, we show that an estimate of the timing error for QOSTBC can be formed by a linear combination of data and decision variable products. Consequently, in contrast to ML-based optimisation techniques, which require computationally intensive likelihood function estimation followed by the search for its maximum, estimators presented here offer very low computational complexity.
- We derive the S-curve for the general form of the estimator, showing that it is independent of the rotation angle ϕ used in the QOSTBC.
- We obtain semi-analytical expressions for the estimation error variance and the TED SNR.
- Symbol-error-rate (SER) performance and the timing error tracking range is evaluated by means of system simulations and compared to the OSTBC TED results reported in [7]. We evaluate the effects of data decision and channel estimation errors for a pilot-symbol-based estimator.

The remainder of this paper is organised as follows. System overview is described in Section 2, while Section 3 presents the theory of TED design and analysis for QOSTBC. System simulations evaluating the performance of QOSTBC receivers incorporating the designed TED are presented in Section 4. We conclude with a summary in Section 5.

2 System overview

Consider an OSTBC system with N_t transmit and N_r receive antennas, where the transmitter encodes N_s information symbols over N_t antennas in N_c time slots, resulting in a code rate of $R = N_s/N_c$. Using boldface notation for matrices, we denote the lth $N_t \times N_c$ code block by $\boldsymbol{X}_l$, and its (i, k)th entry by $x_i(lN_c + k)$. Note that l is the block index, $k = 0, \ldots, N_c - 1$ is the time slot within the block and $i = 1, \ldots, N_t$ is the transmit antenna index. One of the advantages of OSTBC systems lies in the fact that if the columns of $\boldsymbol{X}_l$ are orthogonal, the receiver complexity can be greatly reduced by decoupling the decoding process into N_s independent operations [8]. It has been shown, however, that $N_t = 2$ is the only configuration for which a full rate OSTBC with a complex alphabet is possible, with the maximum rate for $N_t > 2$ is $R = 3/4$ [8]. In order to achieve rate one codes for $N_t > 2$, the property of full code orthogonality must be relaxed, resulting in quasi-OSTBC. An example of a $N_t = 4$ antenna QOSTBC is given by [9]

$$\boldsymbol{X}_{(\text{q4a})} = \begin{bmatrix} a_1 & -a_2^* & -a_3^* & a_4 \\ a_2 & a_1^* & -a_4^* & -a_3 \\ a_3 & -a_4^* & a_1^* & -a_2 \\ a_4 & a_3^* & a_2^* & a_1 \end{bmatrix} \tag{1}$$

where a_m denotes the data symbols. While offering an encoding rate of one, QOSTBCs have been shown [9] to provide only half of the maximum diversity order. To address this shortcoming, a subset of the data symbols can be drawn from a constellation rotated by an angle ϕ, resulting in a ϕ-QOSTBC system [9]. Considering, without loss of generality, the code in (1), we have

$$\tilde{a}_m = \begin{cases} a_m, & m = 1, 2 \\ a_m e^{j\phi}, & m = 3, 4 \end{cases} \quad \tilde{a}_m = \begin{cases} a_m, & m = 1, 2 \\ a_m e^{j\phi}, & m = 3, 4 \end{cases} \tag{2}$$

Using a block index l, the encoding process for the code $\boldsymbol{X}_l$ can be expressed by [10]

$$\boldsymbol{X}_l = \sum_{m=0}^{N_s-1} \Re\{\tilde{a}_{m,l}\}\boldsymbol{A}_m + i\Im\{\tilde{a}_{m,l}\}\boldsymbol{B}_m \tag{3}$$

where the operators $\Re\{\cdot\}$ and $\Im\{\cdot\}$ return the real and imaginary parts of their arguments, respectively, and $\boldsymbol{A}_m$ and $\boldsymbol{B}_m$ are integer code matrices of dimension $N_t \times N_c$.

Following data encoding, the pulse shaping, which is split between the transmitter and the receiver, is performed using root raised cosine (RRC) filters. The combined Nyquist raised cosine pulse is represented by $g(t)$. We assume a frequency-flat Rayleigh fading channel modelled by a $N_r \times N_t$ matrix $\boldsymbol{H}$. Its components, denoted by h_{ji}, correspond to the state of the channel from ith transmit to jth receive antenna and are assumed to be independent and identically distributed (iid) with a U-shaped power spectrum of isotropic scattering and maximum symbol-normalised Doppler frequency of $f_D T$, assumed to be known.

The received signal is sampled with a timing error ε assumed to be equal on all branches and constant for the duration of the one code block $\boldsymbol{X}_l$. Following the model in [7], we consider $\varepsilon = \tau - \hat{\tau}$ where τ is the timing offset at the receiver and $\hat{\tau}$ is the timing correction applied by the timing synchronisation algorithm. Assuming the channel fading is sufficiently slow, such that $h_{ji}(t_n) \simeq h_{ji}(nT) = h_{ji}[n]$, the matched filter samples at receive antenna j are given by

$$y_j[n] = \sum_{i=1}^{N_t} h_{ji}[n] \sum_{n'} x_i[n'] g(nT - n'T + \varepsilon) + \eta_j[n] \tag{4}$$

where $\eta_j[n]$ denotes the samples of the coloured noise resulting from match filtering. Using the same approach as in [7], one can show that the lth $N_r \times N_c$ received matrix $\boldsymbol{Y}_l$ is given by

$$\boldsymbol{Y}_l = \boldsymbol{H}_l \sum_n \boldsymbol{X}_{l+n} \boldsymbol{G}_{\varepsilon,n} + \boldsymbol{N}_l \tag{5}$$

where $\boldsymbol{H}_l$ and $\boldsymbol{N}_l$ denote the channel state and noise matrices, respectively, and $\boldsymbol{G}_{\varepsilon,n}$ is a $N_c \times N_c$ Toeplitz matrix given by

$$\boldsymbol{G}_{\varepsilon,n} = \begin{bmatrix} g^{\varepsilon}_{-nN_c} & g^{\varepsilon}_{-nN_c+1} & g^{\varepsilon}_{-nN_c+2} & \cdots \\ g^{\varepsilon}_{-nN_c-1} & g^{\varepsilon}_{-nN_c} & g^{\varepsilon}_{-nN_c+1} & \ddots \\ g^{\varepsilon}_{-nN_c-2} & g^{\varepsilon}_{-nN_c-1} & g^{\varepsilon}_{-nN_c} & \ddots \\ \vdots & \ddots & \ddots & \ddots \end{bmatrix}$$

where $g^{\varepsilon}_n \triangleq g(nT + \varepsilon)$. The summation in (5) encompasses the effects of intersymbol interference due to ε, where $\boldsymbol{G}_{\varepsilon,\, n} \to 0$ for large $|n|$.

The decoding is accomplished by means of optimisation of a ML metric. Owing to the partial orthogonality properties of the QOSTBCs, the ML metric can be decomposed into a sum of independent terms. Considering once again the code in (1), the metric is given by [9]

$$\mathcal{M} = f_{14}(s_1, s_4) + f_{23}(s_2, s_3) \tag{6}$$

where s_n denotes the nth decision variable. The expressions for $f_{14}(s_1, s_4)$ and $f_{23}(s_2, s_3)$ are derived in [9].

2.1 Channel estimation

In addition to the receiver with perfect channel knowledge, we evaluate the effects of channel estimation errors for a pilot symbol assisted modulation (PSAM) receiver, as described in [2]. The data are divided into frames consisting of known orthogonal pilot blocks, followed by a sequence of OSTBC data code blocks. The received sequence is then decimated to recover the pilot symbols, which are used to obtain the channel estimates for the pilot slots. These are subsequently interpolated to obtain channel fading values for the data portion of each frame.

3 Timing error detector

3.1 Timing error detector design

It was shown in [7] that for an OSTBC system a measurement of ε can be obtained using data symbols (or decisions) and decision variables. The average of the TED output represents the timing error measurement (TEM), referred to as the S-curve. As described in [7], the aim of the design is to obtain, or closely approximate, a TEM in the form of $\hat{\varepsilon} = g^{\varepsilon}_{-1} - g^{\varepsilon}_{1}$. This expression, referred to as the difference of threshold crossings, returns a linear measurement of ε for small values of $|\varepsilon|$. We now show that a similar method can be used to design TEDs for QOSTBC and ϕ-QOSTBC encoding.

doi: 10.1049/iet-com.2012.0244

We note that an OSTBC receiver utilises explicit expressions for the decision variables, which were subsequently used for TEM estimation in [7]. Owing to the fact that the QOSTBC ML decoding in (6) cannot be fully decoupled, no explicit exact decision variables are available for TED design. Thus, in what follows, for the purpose of timing error estimation, we use approximate decision variables which are analogous to the OSTBC expressions, that is

$$\tilde{\zeta}_m = \|\boldsymbol{H}\|^{-2}\left[\Re\left\{\mathrm{tr}\left(\boldsymbol{Y}^H\boldsymbol{H}\boldsymbol{A}_m\right)\right\} - j\Im\left\{\mathrm{tr}\left(\boldsymbol{Y}^H\boldsymbol{H}\boldsymbol{B}_m\right)\right\}\right] \quad (7)$$

One can show that $\tilde{\zeta}_m$ can be expressed as the decision variable s_m with a perturbation δ_{ζ_m}, that is

$$\tilde{\zeta}_m = s_m + \delta_{\zeta_m} \quad (8)$$

where, for the example code in (1), the perturbation terms δ_{ζ_m} are given by [11, Chapter 6]

$$\delta_{\zeta_1} = 2\|\boldsymbol{H}_l\|^{-2}\sum\nolimits_{j=1}^{N_r}\Re\left(h_{j1}h_{j4}^* - h_{j2}^*h_{j3}\right)s_4$$
$$\delta_{\zeta_2} = -2\|\boldsymbol{H}_l\|^{-2}\sum\nolimits_{j=1}^{N_r}\Re\left(h_{j1}h_{j4}^* - h_{j2}^*h_{j3}\right)s_3$$
$$\delta_{\zeta_3} = -2\|\boldsymbol{H}_l\|^{-2}\sum\nolimits_{j=1}^{N_r}\Re\left(h_{j1}h_{j4}^* - h_{j2}^*h_{j3}\right)s_2$$
$$\delta_{\zeta_4} = 2\|\boldsymbol{H}_l\|^{-2}\sum\nolimits_{j=1}^{N_r}\Re\left(h_{j1}h_{j4}^* - h_{j2}^*h_{j3}\right)s_1$$

We note that the numerator of δ_{ζ_m} contains only cross product terms in h_{ji}, whereas the denominator contains magnitude terms. We will show that through the iterative operation of the receiver timing loop, the effect of δ_{ζ_m} will be small, allowing for a valid TEM. While the variables $\tilde{\zeta}_m$ are used for the purpose of TEM estimation, the data decisions s_m are obtained from (6). Finally, the use of (7) allows a semi-analytical derivation of the TED mean and estimation variance.

Similarly to the approach in [7], we consider a general expression for the TED output given by an arbitrary linear combination of products of data symbols and decision variable, that is

$$\hat{\varepsilon} = \Re\left(\sum_k \alpha_k\tilde{a}_{n_{\alpha,k}}\tilde{\zeta}_{m_{\alpha,k}} + \beta_k\tilde{a}_{n_{\beta,k}}^*\tilde{\zeta}_{m_{\beta,k}}\right) \quad (9)$$

with $\tilde{\zeta}_m$ given by (7). The TED design process aims to select the parameter set

$$\mathcal{S} = \left\{\alpha_k, \beta_k, m_{\alpha,k}, n_{\alpha,k}, m_{\beta,k}, n_{\beta,k}\right\} \quad (10)$$

such that the S-curve, that is the average of the TED in (9), is in the form of a difference of threshold crossings TEM $g_{-1}^{\varepsilon} - g_1^{\varepsilon}$. The TED is the input to the timing loop which acts to average (9).

We evaluate the expectation of (9), beginning with the expectation over data and the noise conditioned on the channel response, followed by the expectation over $\boldsymbol{H}$. In order to maintain compact notation, we denote the expectation conditioned on $\boldsymbol{H}$ by $E^{\boldsymbol{H}}\{\cdot\}$, while the expectation over $\boldsymbol{H}$ will be denoted by $E_{\boldsymbol{H}}\{\cdot\}$. Total expectation is thus given by $E\{\cdot\} = E_{\boldsymbol{H}}\{E^{\boldsymbol{H}}\{\cdot\}\}$, where $E_{\boldsymbol{H}}\{\cdot\}$ is always computed by simulation as the argument is too complex for analysis.

Adapting the approach in [7] we evaluate $\Re\{E^{\boldsymbol{H}}\{\tilde{a}_n\tilde{\zeta}_m\}\}$ and $\Re\{E^{\boldsymbol{H}}\{\tilde{a}_n^*\tilde{\zeta}_m\}\}$ in (9). Assuming $E\{a_n^Ra_m^R\} = 0$ for $m \neq n$ and $E\{a_n^Ra_n^I\} = 0$, we can express $\Re\{E^{\boldsymbol{H}}\{\tilde{a}_n\tilde{\zeta}_m\}\}$ as

$$\begin{aligned}\Re\{E^{\boldsymbol{H}}\{\tilde{a}_n\tilde{\zeta}_m\}\} = \|\boldsymbol{H}\|^{-2}\mathrm{tr}\Big\{&\boldsymbol{A}_m\boldsymbol{G}_\varepsilon^H\Big[E\left\{\Re\left(\tilde{a}_n^R\tilde{\boldsymbol{X}}^H\right)\right\}\\ &\times\Re\left(\boldsymbol{H}^H\boldsymbol{H}\right) - E\left\{j\Im\left(\tilde{a}_n^I\tilde{\boldsymbol{X}}^H\right)\right\}\\ &\times\Im\left(\boldsymbol{H}^H\boldsymbol{H}\right)\Big] - j\boldsymbol{B}_m\boldsymbol{G}_\varepsilon^H\Big[E\left\{j\Im\left(\tilde{a}_n^I\tilde{\boldsymbol{X}}^H\right)\right\}\\ &\times\Re\left(\boldsymbol{H}^H\boldsymbol{H}\right) + E\left\{\Re\left(\tilde{a}_n^R\tilde{\boldsymbol{X}}^H\right)\right\}\Im\left(\boldsymbol{H}^H\boldsymbol{H}\right)\Big]\Big\}\end{aligned} \quad (11)$$

Components of (11) can be further evaluated using (3), where one can show that

$$\begin{aligned}\Re\left\{E\left\{\tilde{a}_n^R\tilde{\boldsymbol{X}}^H\right\}\right\} &= \Re\left\{E\left\{\tilde{a}_n^R\sum_{m=0}^{N_s-1}\tilde{a}_m^R\boldsymbol{A}_m^H - j\tilde{a}_m^I\boldsymbol{B}_m^H\right\}\right\}\\ &= E\left\{\left(a_n^R\cos(\phi) - a_n^I\sin(\phi)\right)^2\right\}\boldsymbol{A}_n^H\\ &= \rho_2\boldsymbol{A}_n^H\end{aligned} \quad (12)$$

where ϕ is the rotation angle in (2). In (12) we have assumed $E\{(a_n^R)^2\} = E\{(a_n^I)^2\} = \rho_2$, where ρ_2 is a constellation dependent constant, defined by

$$\rho_p \triangleq E\left\{\left(a_i^R\right)^p\right\} = E\left\{\left(a_i^I\right)^p\right\} \quad (13)$$

Using the same approach, one can show that

$$\Im\left\{E\left\{\tilde{a}_n^I\tilde{\boldsymbol{X}}^H\right\}\right\} = -\rho_2\boldsymbol{B}_n^H \quad (14)$$

Substituting (12) and (14) into (11) and after some algebraic manipulation, taking the real part of (11) results in

$$\begin{aligned}\Re\{E^{\boldsymbol{H}}\{\tilde{a}_n\tilde{\zeta}_m\}\} = \rho_2\|\boldsymbol{H}\|^{-2}&\mathrm{tr}\\ &\times\left\{\left(\boldsymbol{A}_m\boldsymbol{G}_\varepsilon^H\boldsymbol{A}_n^H - \boldsymbol{B}_m\boldsymbol{G}_\varepsilon^H\boldsymbol{B}_n^H\right)\Re\left(\boldsymbol{H}^H\boldsymbol{H}\right)\right\}\end{aligned} \quad (15)$$

Following the development analogous to that in (11)–(15), one can show that $E^{\boldsymbol{H}}\{\tilde{a}_n\tilde{\zeta}_m^*\}$ is given by

$$\begin{aligned}\Re\left\{E^{\boldsymbol{H}}\{\tilde{a}_n^*\tilde{\zeta}_m\}\right\} = \rho_2\|\boldsymbol{H}\|^{-2}&\\ &\times\mathrm{tr}\left\{\left(\boldsymbol{A}_m\boldsymbol{G}_\varepsilon^H\boldsymbol{A}_n^H + \boldsymbol{B}_m\boldsymbol{G}_\varepsilon^H\boldsymbol{B}_n^H\right)\Re\left(\boldsymbol{H}^H\boldsymbol{H}\right)\right\}\end{aligned} \quad (16)$$

We can note that the expressions in (15) and (16) are independent of ϕ. Combining, we have that the S-curve, conditioned on $\boldsymbol{H}$, for a ϕ-QOSTBC TED in (9), is given by an expression identical to that obtained for OSTBCs in [7], that is

$$E^{\boldsymbol{H}}\{\hat{\varepsilon}\} = \rho_2\|\boldsymbol{H}\|^{-2}\mathrm{tr}\left\{\boldsymbol{\Gamma}\Re\left(\boldsymbol{H}^H\boldsymbol{H}\right)\right\} \quad (17)$$

where the matrix $\boldsymbol{\Gamma}$, dependent on $\mathcal{S}$ in (10), is given by

$$\begin{aligned}\boldsymbol{\Gamma} = \sum\nolimits_k\Big[&\alpha_k\left(\boldsymbol{A}_{m_{\alpha,k}}\boldsymbol{G}_\varepsilon^H\boldsymbol{A}_{n_{\alpha,k}}^H - \boldsymbol{B}_{m_{\alpha,k}}\boldsymbol{G}_\varepsilon^H\boldsymbol{B}_{n_{\alpha,k}}^H\right)\\ &+\beta_k\left(\boldsymbol{A}_{m_{\beta,k}}\boldsymbol{G}_\varepsilon^H\boldsymbol{A}_{n_{\beta,k}}^H + \boldsymbol{B}_{m_{\beta,k}}\boldsymbol{G}_\varepsilon^H\boldsymbol{B}_{n_{\beta,k}}^H\right)\Big]\end{aligned} \quad (18)$$

The equivalence of (17) and (18) to the expressions obtained for OSTBC in [7], leads to the conclusion that the TED design conditions for OSTBC are applicable to QOSTBC. Thus, based on the results in [7], if $\boldsymbol{\Gamma}$ satisfies

$$\boldsymbol{\Gamma} = f(\boldsymbol{G}_\varepsilon)\boldsymbol{I} + \boldsymbol{D}$$

where

i. $f(\boldsymbol{G}_\varepsilon)$ is a scalar function of $\boldsymbol{G}_\varepsilon$ returning a difference of threshold crossings (TEM) approximating $g_{-1}^{\varepsilon} - g_{1}^{\varepsilon}$
ii. $\boldsymbol{D}$ is an antisymmetric matrix, then

$$E^{\boldsymbol{H}}\{\hat{\varepsilon}\} = \rho_2 f(\boldsymbol{G}_\varepsilon) \tag{19}$$

Since (19) is independent of $\boldsymbol{H}$, such a TED is robust [7]. If only condition (i) is satisfied, then

$$E^{\boldsymbol{H}}\{\hat{\varepsilon}\} = \rho_2 f(\boldsymbol{G}_\varepsilon) + \delta_{\hat{\varepsilon}} \tag{20}$$

where $\delta_{\hat{\varepsilon}}$, dependent on $\boldsymbol{H}$, is referred to as the TEM bias, which can be shown to be given by

$$\delta_{\hat{\varepsilon}} = \rho_2 \|\boldsymbol{H}\|^{-2} \sum_{m=1}^{N_t} \sum_{i=1 i\neq m}^{N_t} \sum_{j=1}^{N_r} d_{mi} \Re\left(h_{ji}^* h_{jm}\right) \tag{21}$$

where d_{mi} denotes the (m, i)th entry of $\boldsymbol{D}$. The numerator of (21) contains only channel cross product terms, whereas the denominator contains magnitude terms from $\|\boldsymbol{H}\|^2$. Because of the averaging operation of the timing loop, the effect of the bias term will be small, resulting in a quasi-robust TED. For a robust TED, (19) does not require averaging over the $\boldsymbol{H}$, and thus (19) represents the TED S-curve. For a quasi-robust TED, the S-curve is obtained by computing the expectation of the bias $\delta_{\hat{\varepsilon}}$ in (20) over the channel fading matrix $\boldsymbol{H}$, that is

$$E\{\hat{\varepsilon}\} = \rho_2 f(\boldsymbol{G}_\varepsilon) + E_{\boldsymbol{H}}\{\delta_{\hat{\varepsilon}}\} \tag{22}$$

where the expectation $E_{\boldsymbol{H}}\{\delta_{\hat{\varepsilon}}\}$ is evaluated by simulation.

3.2 Estimation error variance

We evaluate the estimation error variance of the TED in (9), given by

$$\sigma_{\hat{\varepsilon}}^2 = E\{\hat{\varepsilon}^2\} - [E\{\hat{\varepsilon}\}]^2 \tag{23}$$

Examining (9), one notes that the solution to $E\{\hat{\varepsilon}^2\}$ can be obtained by considering the expectations $E^{\boldsymbol{H}}\{\tilde{a}_i^R \tilde{a}_j^R \tilde{\zeta}_m^R \tilde{\zeta}_n^R\}$, $E^{\boldsymbol{H}}\{\tilde{a}_i^I \tilde{a}_j^I \tilde{\zeta}_m^I \tilde{\zeta}_n^I\}$ and $E^{\boldsymbol{H}}\{\tilde{a}_i^R \tilde{a}_j^I \tilde{\zeta}_m^R \tilde{\zeta}_n^I\}$, the solution of which is deferred to Appendix. Following the derivation, the expression for $E^{\boldsymbol{H}}\{\tilde{a}_i^R \tilde{a}_j^R \tilde{\zeta}_m^R \tilde{\zeta}_n^R\}$ is given by

$$E^{\boldsymbol{H}}\left\{\tilde{a}_i^R \tilde{a}_j^R \tilde{\zeta}_m^R \tilde{\zeta}_n^R\right\} = \|\boldsymbol{H}\|^{-4} \mathrm{tr}\left\{\rho_2^2 \tilde{\boldsymbol{\Phi}}_{ijmn}^{RR} + \rho_2 \frac{N_0}{2} \tilde{\boldsymbol{\Delta}}_{ijmn}^{RR}\right\} \tag{24}$$

where $\tilde{\boldsymbol{\Phi}}_{ijmn}^{RR}$ is given by (see (25))

and

$$\tilde{\boldsymbol{\Delta}}_{ijmn}^{RR} = \begin{cases} 0 & i \neq j \\ (\boldsymbol{A}_m \otimes \boldsymbol{A}_n)\boldsymbol{\Lambda}_N(\boldsymbol{\Omega}'_{\mathrm{RR}} + \boldsymbol{\Omega}'_{\mathrm{II}}) & i = j \end{cases} \tag{26}$$

where $\boldsymbol{\Omega}_{ij}$ and $\boldsymbol{\Omega}'_{ij}$ are defined in Appendix by (51) and (63), respectively. The $N_c N_c \times N_r N_r$ matrix $\boldsymbol{\Lambda}_N$ is given by (62). In (25), we have defined constellation-dependent constants

$$\rho''_\phi \triangleq E\left\{\left(\tilde{a}_i^R\right)^3 \left(\tilde{a}_i^I\right)\right\}$$

$$\rho'_{2\phi} \triangleq E\left\{\left(\tilde{a}_i^R\right)^2 \left(\tilde{a}_i^I\right)^2\right\}$$

$$\rho_{4\phi} \triangleq E\left\{\left(\tilde{a}_i^R\right)^4\right\}$$

which are evaluated for M-PSK constellations in [11].

Similarly, the solution to $E^{\boldsymbol{H}}\{\tilde{a}_i^I \tilde{a}_j^I \tilde{\zeta}_m^I \tilde{\zeta}_n^I\}$ is given by

$$E^{\boldsymbol{H}}\left\{\tilde{a}_i^I \tilde{a}_j^I \tilde{\zeta}_m^I \tilde{\zeta}_n^I\right\} = \|\boldsymbol{H}\|^{-4} \mathrm{tr}\left\{\rho_2^2 \tilde{\boldsymbol{\Phi}}_{ijmn}^{II} + \rho_2 \frac{N_0}{2} \tilde{\boldsymbol{\Delta}}_{ijmn}^{II}\right\} \tag{27}$$

where (see (28))

$$\tilde{\boldsymbol{\Phi}}_{ijmn}^{RR} = \begin{cases} (\boldsymbol{A}_m \boldsymbol{G}_{\varepsilon,0}^H \otimes \boldsymbol{A}_n \boldsymbol{G}_{\varepsilon,0}^H)\left(\boldsymbol{A}_j^H \otimes \boldsymbol{A}_i^H + \boldsymbol{A}_i^H \otimes \boldsymbol{A}_j^H\right)\boldsymbol{\Omega}_{\boldsymbol{RR}} & i \neq j \\ (\boldsymbol{A}_m \boldsymbol{G}_{\varepsilon,0}^H \otimes \boldsymbol{A}_n \boldsymbol{G}_{\varepsilon,0}^H) \times \left[\left(\frac{\rho_{4\phi}}{\rho_2^2} - 1\right)(\boldsymbol{A}_i^H \otimes \boldsymbol{A}_i^H)\boldsymbol{\Omega}_{\boldsymbol{RR}} + \left(\frac{\rho'_{2\phi}}{\rho_2^2} - 1\right)(\boldsymbol{B}_i^H \otimes \boldsymbol{B}_i^H)\boldsymbol{\Omega}_{\boldsymbol{II}}\right. \\ \left. + \frac{\rho''_\phi}{\rho_2^2}\left((\boldsymbol{A}_i^H \otimes \boldsymbol{B}_i^H)\boldsymbol{\Omega}_{\boldsymbol{RI}} + (\boldsymbol{B}_i^H \otimes \boldsymbol{A}_i^H)\boldsymbol{\Omega}_{\boldsymbol{IR}}\right)\right] \\ + \sum_l \sum_{k=0}^{N_s-1} (\boldsymbol{A}_m \boldsymbol{G}_{\varepsilon,l}^H \otimes \boldsymbol{A}_n \boldsymbol{G}_{\varepsilon,l}^H) \times \left[(\boldsymbol{A}_k^H \otimes \boldsymbol{A}_k^H)\boldsymbol{\Omega}_{\boldsymbol{RR}} + (\boldsymbol{B}_k^H \otimes \boldsymbol{B}_k^H)\boldsymbol{\Omega}_{\boldsymbol{II}}\right] & i = j \end{cases} \tag{25}$$

$$\tilde{\boldsymbol{\Phi}}_{ijmn}^{II} = \begin{cases} (\boldsymbol{B}_m \boldsymbol{G}_{\varepsilon,0}^H \otimes \boldsymbol{B}_n \boldsymbol{G}_{\varepsilon,0}^H)\left(\boldsymbol{B}_j^H \otimes \boldsymbol{B}_i^H + \boldsymbol{B}_i^H \otimes \boldsymbol{B}_j^H\right)\boldsymbol{\Omega}_{RR} & i \neq j \\ (\boldsymbol{B}_m \boldsymbol{G}_{\varepsilon,0}^H \otimes \boldsymbol{B}_n \boldsymbol{G}_{\varepsilon,0}^H) \times \left[\left(\frac{\rho_{4\phi}}{\rho_2^2} - 1\right)(\boldsymbol{B}_i^H \otimes \boldsymbol{B}_i^H)\boldsymbol{\Omega}_{RR} + \left(\frac{\rho'_{2\phi}}{\rho_2^2} - 1\right)(\boldsymbol{A}_i^H \otimes \boldsymbol{A}_i^H)\boldsymbol{\Omega}_{\mathrm{II}}\right. \\ \left. - \frac{\rho''_\phi}{\rho_2^2}\left((\boldsymbol{A}_i^H \otimes \boldsymbol{B}_i^H)\boldsymbol{\Omega}_{\mathrm{IR}} + (\boldsymbol{B}_i^H \otimes \boldsymbol{A}_i^H)\boldsymbol{\Omega}_{\mathrm{RI}}\right)\right] \\ + \sum_l \sum_{k=0}^{N_s-1} (\boldsymbol{B}_m \boldsymbol{G}_{\varepsilon,l}^H \otimes \boldsymbol{B}_n \boldsymbol{G}_{\varepsilon,l}^H) \times \left[(\boldsymbol{B}_k^H \otimes \boldsymbol{B}_k^H)\boldsymbol{\Omega}_{RR} + (\boldsymbol{A}_k^H \otimes \boldsymbol{A}_k^H)\boldsymbol{\Omega}_{\mathrm{II}}\right] & i = j \end{cases} \tag{28}$$

doi: 10.1049/iet-com.2012.0244

and

$$\tilde{\boldsymbol{\Delta}}^{II}_{ijmn} = \begin{cases} 0, & i \neq j \\ (\boldsymbol{B}_m \otimes \boldsymbol{B}_n)\boldsymbol{\Lambda}_N(\boldsymbol{\Omega}'_{\mathrm{RR}} + \boldsymbol{\Omega}'_{\mathrm{II}}), & i = j \end{cases} \quad (29)$$

Finally, the expectation $E^{\boldsymbol{H}}\left\{\tilde{a}_i^R \tilde{a}_j^I \tilde{\zeta}_m^R \tilde{\zeta}_n^I\right\}$ is given by

$$E^{\boldsymbol{H}}\left\{\tilde{a}_i^R \tilde{a}_j^I \tilde{\zeta}_m^R \tilde{\zeta}_n^I\right\} = \|\boldsymbol{H}\|^{-4}\mathrm{tr}\left\{\mu_\phi \tilde{\boldsymbol{\Phi}}^{RI}_{ijmn}\right\} \quad (30)$$

where

$$\tilde{\boldsymbol{\Phi}}^{RI}_{ijmn} = \left(\boldsymbol{A}_m \boldsymbol{G}^H_{\varepsilon,0} \otimes \boldsymbol{B}_n \boldsymbol{G}^H_{\varepsilon,0}\right) \times \left(\left(\boldsymbol{A}_i^H \otimes \boldsymbol{B}_j^H\right)\boldsymbol{\Omega}_{\mathrm{RR}} - \left(\boldsymbol{B}_j^H \otimes \boldsymbol{A}_i^H\right)\boldsymbol{\Omega}_{\mathrm{II}}\right) \quad (31)$$

and μ_ϕ is defined as

$$\mu_\phi = \begin{cases} \rho_2^2, & i \neq j \\ \rho'_{2\phi}, & i = j \end{cases}$$

Using the general results given by (24), (27) and (30), the estimation variance for a particular TED is obtained using (23) with $E\{\hat{\varepsilon}\}$ computed via (17) and (18). Combining, we obtain

$$E\left\{\hat{\varepsilon}^2\right\} = E_{\boldsymbol{H}}\left\{\|\boldsymbol{H}\|^{-4}\mathrm{tr}\left\{\rho_2^2 \boldsymbol{\Sigma}_{\tilde{\boldsymbol{\Phi}}} + \rho_2 \frac{N_0}{2}\boldsymbol{\Sigma}_{\tilde{\boldsymbol{\Delta}}}\right\}\right\} \quad (32)$$

The expectation $E_{\boldsymbol{H}}\{\cdot\}$ must be carried out by simulation, as will be done in Section 3.4. The quantities $\boldsymbol{\Sigma}_{\tilde{\boldsymbol{\Phi}}}$ and $\boldsymbol{\Sigma}_{\tilde{\boldsymbol{\Delta}}}$ correspond to the linear combinations of $\tilde{\boldsymbol{\Phi}}^{RR}_{ijmn}$, $\tilde{\boldsymbol{\Phi}}^{II}_{ijmn}$, $\tilde{\boldsymbol{\Phi}}^{RI}_{ijmn}$ (defined by (25), (28) and (31)) and $\tilde{\boldsymbol{\Delta}}^{RR}_{ijmn}$, $\tilde{\boldsymbol{\Delta}}^{II}_{ijmn}$ (defined by (26) and (29)), respectively, as determined by the polynomial expansion of $E\left\{\hat{\varepsilon}^2\right\}$ for a particular TED.

Comparing the estimation error variance results with those obtained in [7] for OSTBC TEDs, one can notice that the expressions for $\tilde{\boldsymbol{\Phi}}^{RR}_{ijmn}$ and $\tilde{\boldsymbol{\Phi}}^{II}_{ijmn}$ in (25) and (28) contain additional terms resulting from the constellation rotation angle ϕ.

Unlike the S-curve for ϕ-QOSTBC, the estimation variance is a function of the rotation angle ϕ. This is, however, only the case for $\tilde{\boldsymbol{\Phi}}^{RR}_{ijmn}$, $\tilde{\boldsymbol{\Phi}}^{II}_{ijmn}$, $\tilde{\boldsymbol{\Phi}}^{RI}_{ijmn}$ of $\boldsymbol{\Sigma}_{\tilde{\boldsymbol{\Phi}}}$ where $i = j$ and where i refers to the data symbol from a rotated constellation. While an exhaustive search considering all known QOSTBCs has not been performed, all of the valid TED expressions obtained by the authors were depended strictly on data from non-rotated constellations. Thus, the corresponding estimation error variance expressions were in all cases independent of ϕ. It is possible, however, that there exist TED expressions whose error variance is a function of ϕ.

Finally, using (22) and (23), we define the TED SNR as

$$\mathrm{SNR}_{\mathrm{TED}} = \frac{E^2\{\hat{\varepsilon}\}}{\sigma^2_{\hat{\varepsilon}}} \quad (33)$$

3.3 TED examples

In this section, we consider two specific $N_t = 4$ QOSTBCs. First, consider code $\boldsymbol{X}_{(q4a)}$ defined by (1). More examples of TED expressions can be found in [11, Chapter 6]. The TEM function for $\boldsymbol{X}_{(q4a)}$ can be obtained from the average of the simple combining rule

$$\begin{aligned}\hat{\varepsilon}_{(q4a)} &= \Re\left(a_0\zeta_1 - a_1\zeta_0\right) \\ &= a_0^R\zeta_1^R - a_0^I\zeta_1^I - a_1^R\zeta_0^R + a_1^I\zeta_0^I\end{aligned} \quad (34)$$

The TED in (34) corresponds to $\mathcal{S}$ in (10) with $\beta_k = 0\ \forall k$, $\alpha_1 = -\alpha_2 = 1$, $n_{\alpha,1} = m_{\alpha,2} = 0$, $m_{\alpha,1} = n_{\alpha,2} = 1$.

Substituting the values of $\mathcal{S}$ into (18) and carrying out the matrix multiplications gives $\boldsymbol{\Gamma}$ in the form of

$$\boldsymbol{\Gamma}_{(q4a)} = 2\begin{bmatrix} g^\varepsilon_{-1} - g^\varepsilon_1 & 0 & 0 & -2g^\varepsilon_{-2} \\ 0 & g^\varepsilon_{-1} - g^\varepsilon_1 & 2g^\varepsilon_{-2} & 0 \\ 0 & -2g^\varepsilon_2 & g^\varepsilon_{-1} - g^\varepsilon_1 & 0 \\ 2g^\varepsilon_2 & 0 & 0 & g^\varepsilon_{-1} - g^\varepsilon_1 \end{bmatrix} \quad (35)$$

Examining $\boldsymbol{\Gamma}_{(q4a)}$ in (35), we note that the matrix does not fully satisfy the antisymmetry condition, and hence the resulting TED will be quasi-robust, with the S-curve given by

$$E\left\{\hat{\varepsilon}_{(q4a)}\right\} = 2\rho_2\left(g^\varepsilon_{-1} - g^\varepsilon_1\right) + E_{\boldsymbol{H}}\left\{\delta_{\hat{\varepsilon}_{(q4a)}}\right\} \quad (36)$$

and a TEM bias of

$$\delta_{\hat{\varepsilon}_{(q4a)}} = 2\|\boldsymbol{H}\|^{-2}\rho_2\sum_{j=1}^{N_r}\left[2\left(g^\varepsilon_{-2} - g^\varepsilon_2\right)\Re\left(h^*_{2j}h_{3j} + h^*_{1j}h_{4j}\right)\right] \quad (37)$$

which, as explained in Section 3.1, is small.

To evaluate the TEM estimation variance, we solve $E^{\boldsymbol{H}}\left\{\hat{\varepsilon}^2\right\}$ using (32) by first obtaining the components of $\boldsymbol{\Sigma}_{\tilde{\boldsymbol{\Phi}}}$ and $\boldsymbol{\Sigma}_{\tilde{\boldsymbol{\Delta}}}$, which in turn is done by computing $\hat{\varepsilon}^2$ from (34). Squaring (34) will lead to $\boldsymbol{\Sigma}_{\tilde{\boldsymbol{\Phi}}}$ in the form of

$$\begin{aligned}\boldsymbol{\Sigma}_{\tilde{\boldsymbol{\Phi}}} = {} & \tilde{\boldsymbol{\Phi}}^{RR}_{1100} + \tilde{\boldsymbol{\Phi}}^{RR}_{0011} - 2\tilde{\boldsymbol{\Phi}}^{RR}_{1010} + \tilde{\boldsymbol{\Phi}}^{II}_{1100} + \tilde{\boldsymbol{\Phi}}^{II}_{0011} \\ & - 2\tilde{\boldsymbol{\Phi}}^{II}_{1010} - 2\tilde{\boldsymbol{\Phi}}^{RI}_{1100} - 2\tilde{\boldsymbol{\Phi}}^{RI}_{0011} + 2\tilde{\boldsymbol{\Phi}}^{RI}_{1001} + 2\tilde{\boldsymbol{\Phi}}^{RI}_{0110}\end{aligned} \quad (38)$$

where $\tilde{\boldsymbol{\Phi}}^{RR}_{ijmn}$, $\tilde{\boldsymbol{\Phi}}^{II}_{ijmn}$ and $\tilde{\boldsymbol{\Phi}}^{RI}_{ijmn}$ are defined by (25), (28) and (31), respectively. Similarly, the quantity $\boldsymbol{\Sigma}_{\tilde{\boldsymbol{\Delta}}}$ for $\boldsymbol{X}_{(q4a)}$ is given by

$$\boldsymbol{\Sigma}_{\tilde{\boldsymbol{\Delta}}} = \tilde{\boldsymbol{\Delta}}^{RR}_{1100} + \tilde{\boldsymbol{\Delta}}^{RR}_{0011} + \tilde{\boldsymbol{\Delta}}^{II}_{1100} + \tilde{\boldsymbol{\Delta}}^{II}_{0011} \quad (39)$$

with $\tilde{\boldsymbol{\Delta}}^{RR}_{ijmn}$ and $\tilde{\boldsymbol{\Delta}}^{II}_{ijmn}$ defined by (26) and (29), respectively. We note that since only indices of data drawn from the non-rotated constellation are present, the variance for $\boldsymbol{X}_{(q4a)}$ will be independent of ϕ.

As a second example, we consider a QOSTBC [9]

$$\boldsymbol{X}_{(q4b)} = \begin{bmatrix} a_1 & -a_2^* & a_3 & -a_4^* \\ a_2 & a_1^* & a_4 & a_3^* \\ a_3 & -a_4^* & a_1 & -a_2^* \\ a_4 & a_3^* & a_2 & a_1^* \end{bmatrix} \tag{40}$$

For the $\boldsymbol{X}_{(q4b)}$, a quasi-robust TED can be formed using the same expression as for (34), that is

$$\hat{\varepsilon}_{(q4b)} = \Re\left(a_0\zeta_1 - a_1\zeta_0\right) \tag{41}$$

One can show that the resulting $\boldsymbol{\Gamma}$ is given by

$$\boldsymbol{\Gamma}_{(q4b)} = 2\begin{bmatrix} g_{-1}^{\varepsilon} - g_1^{\varepsilon} & 0 & g_1^{\varepsilon} - g_3^{\varepsilon} & 0 \\ 0 & g_{-1}^{\varepsilon} - g_1^{\varepsilon} & 0 & g_1^{\varepsilon} - g_3^{\varepsilon} \\ g_{-3}^{\varepsilon} - g_{-1}^{\varepsilon} & 0 & g_{-1}^{\varepsilon} - g_1^{\varepsilon} & 0 \\ 0 & g_{-3}^{\varepsilon} - g_{-1}^{\varepsilon} & 0 & g_{-1}^{\varepsilon} - g_1^{\varepsilon} \end{bmatrix} \tag{42}$$

which corresponds to an S-curve given by

$$E\left\{\hat{\varepsilon}_{(q4b)}\right\} = 2\rho_2\left(g_{-1}^{\varepsilon} - g_1^{\varepsilon}\right) + E_{\boldsymbol{H}}\left\{\delta_{\hat{\varepsilon}_{(q4b)}}\right\} \tag{43}$$

and a TEM bias of

$$\delta_{\hat{\varepsilon}_{(q4b)}} = 2\|\boldsymbol{H}\|^{-2}\rho_2 \times \sum_{j=1}^{N_r}\left[2\left(g_1^{\varepsilon} - g_{-1}^{\varepsilon} - g_3^{\varepsilon} + g_{-3}^{\varepsilon}\right)\Re\left(h_{j1}^* h_{j3} + h_{j2}^* h_{j4}\right)\right] \tag{44}$$

The estimation variance for $\boldsymbol{X}_{(q4b)}$ is computed in a manner identical to that for $\boldsymbol{X}_{(q4a)}$. Since the expression for $\hat{\varepsilon}_{(q4b)}$ is identical to that for $\hat{\varepsilon}_{(q4a)}$, the components of $\boldsymbol{\Sigma}_{\tilde{\boldsymbol{\Phi}}}$ and $\boldsymbol{\Sigma}_{\tilde{\boldsymbol{\Delta}}}$ are the same, that is given by (38) and (39). We note that the components of $\boldsymbol{\Sigma}_{\tilde{\boldsymbol{\Phi}}}$ and $\boldsymbol{\Sigma}_{\tilde{\boldsymbol{\Delta}}}$, which depend on the code matrices $\boldsymbol{A}$ and $\boldsymbol{B}$, will have different values.

3.4 Properties of example TED

Fig. 1 shows the S-curve for $\hat{\varepsilon}_{(q4a)}$. The results include the data-aided, semi-analytical expression in (36), with the expectation over the bias (37) computed numerically. We verify the theoretical expression by means of simulation, where the data were sampled with a fixed timing offset and the receiver timing loop is disabled. The S-curve was obtained by averaging $\hat{\varepsilon}$ over all code blocks transmitted. In addition, a simulated decision-directed S-curve was plotted to evaluate the effects of incorrect data decisions. The effect of data decision errors was evaluated by replacing the data symbols in (34) by their corresponding data decisions for SNR $\bar{E}_s/N_0 = 10$ dB and 20 dB, where $\bar{E}_s$ and N_0 denote the average symbol energy, and the noise power spectral density, respectively. The simulations were done for $N_r = 1$ and $N_r = 4$ receive branches.

As indicated by Fig. 1, in the case of a data-aided TED, the simulated results follow the theoretical expressions very closely. By examining the decision-directed S-curve, we note that the incorrect data decisions reduce the linear estimation region to approximately $|\varepsilon|/T \simeq 0.20$ for SNR of 20 dB, with the range extended to $|\varepsilon|/T \simeq 0.30$ with increased diversity order. While the linear estimation range

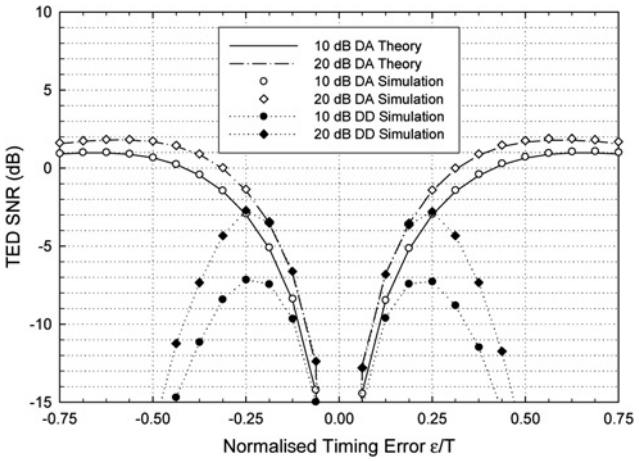

Fig. 2 *TED SNR ($N_t = 4$, $N_r = 1$, SNR = 10, 20 dB)*

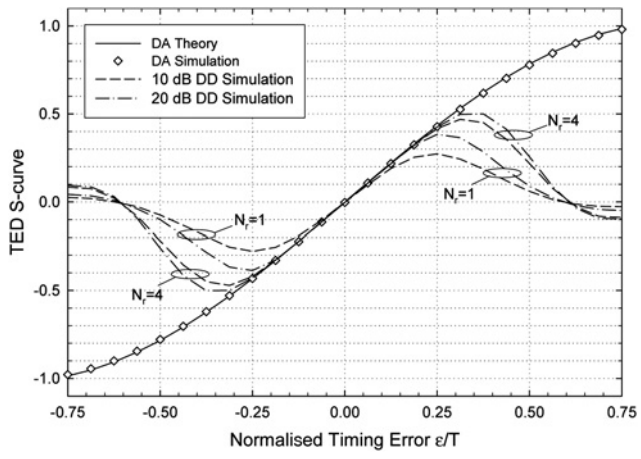

Fig. 1 *TED S-curve ($N_t = 4$, $N_r = 1,4$, SNR = 10, 20 dB)*

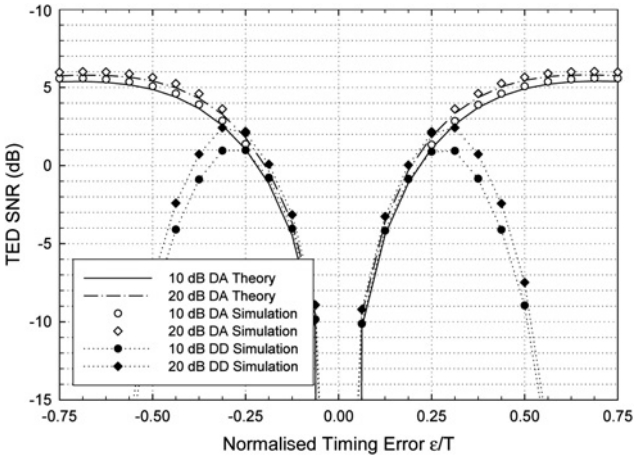

Fig. 3 *TED SNR ($N_t = 4$, $N_r = 4$, SNR = 10, 20 dB)*

doi: 10.1049/iet-com.2012.0244

in Fig. 1 is sufficient for timing loop operation, it is approximately 20% smaller than that for OSTBC TEDs [7]. This can be attributed to the use of approximate decision variables in (7) in timing estimation.

Figs. 2 and 3 show the corresponding plots for TED SNR, computed using (33), with $N_r = 1$ and $N_r = 4$ receive antennas, respectively. The numerator in (33) was obtained using the same methodology as the results in Fig. 1. For the semi-analytical results, $\sigma^2_{\hat{\varepsilon}}$ was computed using (32) with (38) and (39), with numerical averaging over $\boldsymbol{H}$. In the case of the simulated results (data-aided and decision-directed), we average $(\varepsilon - \hat{\varepsilon})^2$ over all code blocks transmitted, with fixed, uncompensated timing error.

Examining Figs. 2 and 3, we note that, similarly to the S-curve, the simulated DA and analytical results are in close agreement. In the case of the data-decision operation, we observe a drop in the TED-SNR corresponding to the non-linear region of the S-curve. Comparing Figs. 2 and 3 to the corresponding results in [7] we find that the peak DD TED SNR is 1.9 dB and 1.5 dB lower for $\bar{E}_s/N_0 = 10$ dB and $\bar{E}_s/N_0 = 20$ dB, respectively, when comparing to TED for $N_t = 4$ TED. Similarly to the reduction in S-curve linearity, we attribute this performance degradation to the decision variable perturbation in (8).

Finally, we should note that the property evaluated in Fig. 3 is the output SNR of the TED, which constitutes the input SNR of the timing loop. Since the timing loop performs an averaging operation by virtue of the loop filter and the threshold device, the TED SNR will be significantly increased by virtue of the integration process.

4 System simulations

We present the simulation results evaluating the tracking performance of receiver employing the TED $\hat{\varepsilon}_{(q4a)}$ applied to QOSTBC in (1) with quadrature phase shift keying (QPSK) modulation and an optimal rotation angle of $\phi = \pi/4$ [9]. In order to provide an accurate comparison to the results in [7], the same simulation setup and parameters are used. Specifically, we consider frequency-flat Rayleigh fading with a normalised Doppler frequency of $f_D T = 0.01$. It is assumed that the receiver has performed coarse timing acquisition, which would be typically done via a training sequence. The timing drift was simulated by perturbing the sampling phase τ_l, where the interval between timing slips, measured in symbol intervals and denoted by N_τ, was modelled by a Gaussian random variable, with a mean of $\bar{N}_\tau$ and a variance $\sigma^2_{N_\tau} = 0.1\bar{N}_\tau$. The drift direction was random and equiprobable, and the step size was fixed to $T/16$. The mean normalised timing error bandwidth is thus given by

$$\bar{B}_\tau T = \frac{T/16}{\bar{N}_\tau T} = \frac{1}{16\bar{N}_\tau}$$

The timing estimation was done using the TED given by (34). Since the focus of the investigation is to track the performance of the detector, the timing estimation was done without the data knowledge at the receiver. Hence the data symbols a_m in (34) were replaced by their estimates $\hat{a}_m$. The timing error estimate for code block l, that is $\hat{\varepsilon}_l$, was passed through a first-order, IIR, timing loop filter with the output of

$$\hat{\varepsilon}'_l = \alpha\hat{\varepsilon}'_{l-1} + (1-\alpha)\hat{\varepsilon}_l$$

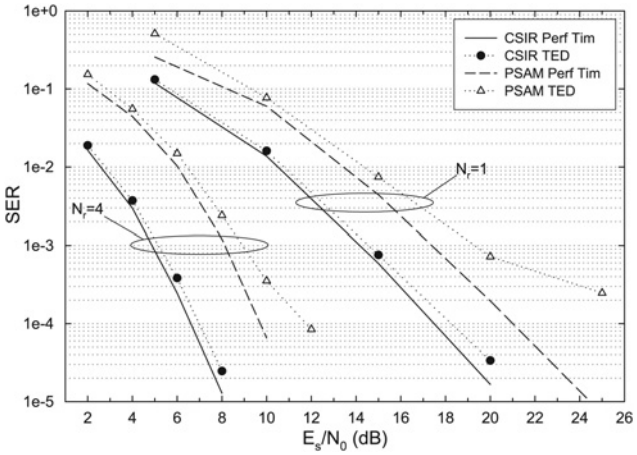

Fig. 4 *QPSK SER performance ($N_t = 4$, $N_r = 1,4$, $B_\tau T = 10^{-4}$)*

where the loop constant $\alpha = 0.9$. When $\hat{\varepsilon}'_l$ exceeded a threshold value $\varepsilon_{\text{th}} = 0.25$, the timing correction $\hat{\tau}_l$ was adjusted by a fraction of the symbol interval $T/8$, according to the polarity of the error estimate. In practice, this can be implemented using a bank of polyphase filters [12].

To evaluate the sensitivity of the algorithm on channel estimation errors, as outlined in Section 2.1, we include the results of PSAM transmission with orthogonal pilots, inserted every four OSTBC data blocks. Wiener interpolation filter with nine interpolants was used.

Fig. 4 presents the SER performance using timing drift bandwidth. The state-of-the-art temperature compensated crystal oscillators have a frequency stability of well under 10 ppm, corresponding to $\bar{B}_\tau T < 10^{-5}$ [13]. $\bar{B}_\tau T = 10^{-4}$. The results for channel state information at the receiver (CSIR) and PSAM receivers are presented, in addition to reference curves for perfect channel and timing estimation, and perfect timing with PSAM channel estimation.

The results demonstrate that the CSIR receiver, which was assumed in the TED design process, is able to track the timing variation with a performance drop of approximately 0.5 dB. Comparing with the results for

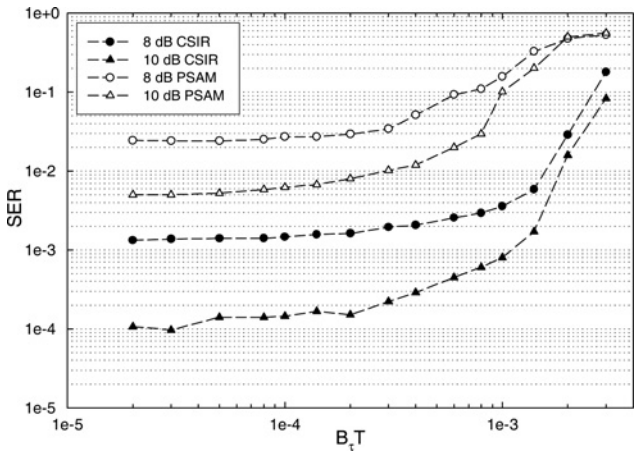

Fig. 5 *QPSK SER performance against timing drift bandwidth ($N_t = 4$, $N_r = 2$)*

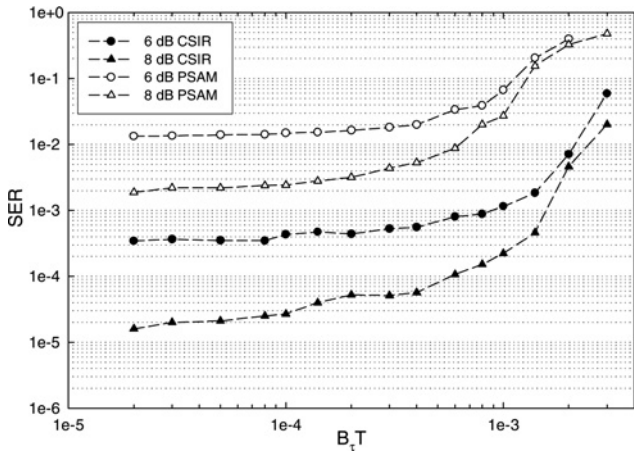

Fig. 6 *QPSK SER performance against timing drift bandwidth ($N_t = 4$, $N_r = 4$)*

OSTBC in [7], this represents a loss of approximately 0.2 dB. In the case of PSAM receiver, the SER performance exhibits degradation in the high SER region, not reported for OSTBC in [7]. In the case of QOSTBC results in Fig. 4, by observing the reference curves for perfect timing with PSAM channel estimation, we note that the TED performance is sensitive to the channel estimation errors. Since the performance for the CSIR receiver is very good, we conclude that improved channel estimation technique should be considered.

With the aim of determining the tracking capabilities of the proposed receiver for varying rates of timing drift, we now consider SER performance as a function of $B_\tau T$. Figs. 5 and 6 show the results for $N_r = 2$ and $N_r = 4$ receivers, respectively, both with CSIR and PSAM.

We note that in the case of CSIR, the timing loop tracks the timing drift up to $B_\tau T \simeq 10^{-3}$, at which point we observe a steep increase in the SER as a result of bursts of errors due to loss of synchronisation. The presence of the channel estimation errors in PSAM causes a reduction in the tracking range to $B_\tau T \simeq 4 \times 10^{-3}$. Comparing these results with those reported for OSTBC in [7], we note that the errors introduced by the decision variables perturbation in (8) act to reduce the tracking range, with the effect being more pronounced for PSAM, where for $N_t = 2$ the loss of synchronisation drops from $B_\tau T \simeq 10^{-3}$ to $B_\tau T \simeq 4 \times 10^{-3}$.

5 Conclusion

We have presented the design and analysis of QOSTBC TEDs, showing that a low-complexity timing measurement can be obtained by operating on data symbols and approximate decision variables. The S-curve, estimation variance and TED SNR were solved under ideal conditions of perfect data and channel state knowledge at the receiver. The simulation results were used to analyse the above properties with decision errors, and to evaluate the system performance including the effects of channel estimation. SER results showed a timing synchronisation loss of CSIR under 0.5 dB. Simulations revealed that the receiver is able to track timing drift bandwidth of $B_\tau T \simeq 10^{-3}$ and $B_\tau T \simeq 4 \times 10^{-3}$ for CSIR and PSAM, respectively.

6 Acknowledgment

The author wishes to thank Professor (Emeritus) Peter J. McLane for his invaluable input during the early stages of this work. Portions of this work were presented at Wireless Communications and Networking Conference (WCNC), 2007.

7 References

1 Dmochowski, P.A., McLane, P.J.: 'Timing synchronization for quasi-orthogonal space–time block coding receivers'. Proc. IEEE Wireless Communications and Networking Conf. (WCNC), September 2007, pp. 1166–1171
2 Naguib, A.F., Tarokh, V., Seshadri, N., Calderbank, R.: 'A space–time coding modem for high-data-rate wireless communications', *IEEE J. Sel. Areas Commun.*, 1998, **16**, (8), pp. 1459–1478
3 Wu, Y.-C., Chan, S.C., Serpedin, E.: 'Symbol-timing synchronization in space–time coding systems using orthogonal training sequences'. Proc. IEEE WCNC, March 2004, pp. 1205–1209
4 Rajawat, K., Chaturvedi, A.K.: 'A low complexity symbol timing estimator for MIMO systems using two samples per symbol', *IEEE Commun. Lett.*, 2006, **10**, (7), pp. 525–527
5 Li, X., Wu, Y.-C., Serpedin, E.: 'Timing synchronization in decode-and-forward cooperative communication systems', *IEEE Trans. Signal Process.*, 2009, **57**, (4), pp. 1444–1455
6 Wang, C.-L., Wang, H.-C.: 'Optimized joint fine timing synchronization and channel estimation for MIMO systems', *IEEE Trans. Commun.*, 2011, **59**, (4), pp. 1089–1098
7 Dmochowski, P.A., McLane, P.J.: 'Timing error detector design and analysis for orthogonal space–time block code receivers', *IEEE Trans. Commun.*, 2008, **56**, (11), pp. 1939–1949
8 Tarokh, V., Jafarkhani, H., Calderbank, A.R.: 'Space–time block codes from orthogonal designs', *IEEE Trans. Inf. Theory*, 1999, **45**, pp. 1456–1467
9 Jafarkhani, H.: 'Space–time coding – theory and practice' (Cambridge University Press, New York, 2005)
10 Ganesan, G., Stoica, P.: 'Space–time block codes: a maximum SNR approach', *IEEE Trans. Inf. Theory*, 2001, **47**, (4), pp. 1650–1656
11 Dmochowski, P.A.: 'Timing synchronization for multiple input multiple output communication system'. PhD thesis, Queen's University, Kingston, ON, Canada, 2006
12 Harris, F.J., Rice, M.: 'Multirate digital filters for symbol timing synchronization in software defined radios', *IEEE J. Sel. Areas Commun.*, 2001, **19**, (12), pp. 2346–2357
13 Zhou, W., Zhou, H., Xuan, Z., Zhang, W.: 'Comparison among precision temperature compensated crystal oscillators'. Proc. IEEE Int. Frequency Control Symp. and Exposition, August 2005, pp. 575–579
14 Horn, R.A., Johnson, C.R.: 'Topics in matrix analysis' (Cambridge University Press, 1991)

8 Appendix 1

8.1 TED variance

We derive the expression for $E^{\boldsymbol{H}}\left\{\tilde{a}_i^R \tilde{a}_j^R \tilde{\zeta}_m^R \tilde{\zeta}_n^R\right\}$ in (24) used in computing the estimation error variance for TED in (9). The equivalent solutions for $E^{\boldsymbol{H}}\left\{\tilde{a}_i^I \tilde{a}_j^I \tilde{\zeta}_m^I \tilde{\zeta}_n^I\right\}$ and $E^{\boldsymbol{H}}\left\{\tilde{a}_i^R \tilde{a}_j^I \tilde{\zeta}_m^R \tilde{\zeta}_n^I\right\}$ can easily be obtained using the same methodology as presented herein. The derivation is an adaptation of that for OSTBC [7], with additional complexity due to the rotation of data symbols. For more details, the readers are referred to [11].

We begin by expanding $E^{\boldsymbol{H}}\left\{\tilde{a}_i^R \tilde{a}_j^R \tilde{\zeta}_m^R \tilde{\zeta}_n^R\right\}$ using (5) and (7). Using the fact that $\mathrm{tr}(\boldsymbol{A})\mathrm{tr}(\boldsymbol{B}) = \mathrm{tr}(\boldsymbol{A} \otimes \boldsymbol{B})$ [14, p.250], we have

doi: 10.1049/iet-com.2012.0244

the solution given by

$$E^{\boldsymbol{H}}\left\{\tilde{a}_i^R\tilde{a}_j^R\tilde{\zeta}_m^R\tilde{\zeta}_n^R\right\} = \|\boldsymbol{H}\|^{-4}E^{\boldsymbol{H}}\Bigg\{\tilde{a}_i^R\tilde{a}_j^R \times \mathrm{tr}\Bigg[\sum_l \boldsymbol{A}_m\boldsymbol{G}_{\varepsilon,l}^H\Re\left(\tilde{\boldsymbol{X}}_l^H\boldsymbol{H}^H\boldsymbol{H}\right) \otimes \sum_{l'}\boldsymbol{A}_n\boldsymbol{G}_{\varepsilon,l'}^H\Re\left(\tilde{\boldsymbol{X}}_{l'}^H\boldsymbol{H}^H\boldsymbol{H}\right) + \boldsymbol{A}_m\Re\left(\boldsymbol{N}^H\boldsymbol{H}\right)\otimes\boldsymbol{A}_n\Re\left(\boldsymbol{N}^H\boldsymbol{H}\right) + \sum_l \boldsymbol{A}_m\boldsymbol{G}_{\varepsilon,l}^H\Re\left(\tilde{\boldsymbol{X}}_l^H\boldsymbol{H}^H\boldsymbol{H}\right) \otimes \boldsymbol{A}_n\Re\left(\boldsymbol{N}^H\boldsymbol{H}\right) + \boldsymbol{A}_m\Re\left(\boldsymbol{N}^H\boldsymbol{H}\right) \otimes \sum_l \boldsymbol{A}_n\boldsymbol{G}_{\varepsilon,l}^H\Re\left(\tilde{\boldsymbol{X}}_l^H\boldsymbol{H}^H\boldsymbol{H}\right)\Bigg]\Bigg\} \quad (45)$$

We note that the expectation of the last two arguments of the trace operator in (45) is zero, since the noise is assumed to be zero-mean and independent of data and code blocks $\tilde{\boldsymbol{X}}_l$. Thus, we can simplify (45) to

$$E^{\boldsymbol{H}}\left\{\tilde{a}_i^R\tilde{a}_j^R\tilde{\zeta}_m^R\tilde{\zeta}_n^R\right\} = \|\boldsymbol{H}\|^{-4}E^{\boldsymbol{H}}\left\{\tilde{a}_i^R\tilde{a}_j^R\mathrm{tr}\left(\tilde{\boldsymbol{\Psi}}_X^{RR} + \tilde{\boldsymbol{\Psi}}_N^{RR}\right)\right\} \quad (46)$$

where $\tilde{\boldsymbol{\Psi}}_X^{RR}$ and $\tilde{\boldsymbol{\Psi}}_N^{RR}$ are defined by

$$\tilde{\boldsymbol{\Psi}}_X^{RR} = \sum_l \boldsymbol{A}_m\boldsymbol{G}_{\varepsilon,l}^H\Re\left(\tilde{\boldsymbol{X}}_l^H\boldsymbol{H}^H\boldsymbol{H}\right)\otimes \times \sum_{l'}\boldsymbol{A}_n\boldsymbol{G}_{\varepsilon,l'}^H\Re\left(\tilde{\boldsymbol{X}}_{l'}^H\boldsymbol{H}^H\boldsymbol{H}\right) \quad (47)$$

and

$$\tilde{\boldsymbol{\Psi}}_N^{RR} = \boldsymbol{A}_m\Re\left(\boldsymbol{N}^H\boldsymbol{H}\right)\otimes\boldsymbol{A}_n\Re\left(\boldsymbol{N}^H\boldsymbol{H}\right) \quad (48)$$

For zero mean data, the expectation of the term in (46) involving $\tilde{\boldsymbol{\Psi}}_X^{RR}$ will contribute only to $l = l'$ summation terms. We can thus write

$$E^{\boldsymbol{H}}\left\{\tilde{a}_i^R\tilde{a}_j^R\mathrm{tr}\left(\tilde{\boldsymbol{\Psi}}_X^{RR}\right)\right\} = \mathrm{tr}\Bigg\{\sum_l\left(\boldsymbol{A}_m\boldsymbol{G}_{\varepsilon,l}^H\otimes\boldsymbol{A}_n\boldsymbol{G}_{\varepsilon,l}^H\right) \times E^{\boldsymbol{H}}\left\{\tilde{a}_i^R\tilde{a}_j^R\Re\left(\tilde{\boldsymbol{X}}_l^H\boldsymbol{H}^H\boldsymbol{H}\right) \otimes\Re\left(\tilde{\boldsymbol{X}}_l^H\boldsymbol{H}^H\boldsymbol{H}\right)\right\}\Bigg\} \quad (49)$$

which can be further expanded resulting in

$$E^{\boldsymbol{H}}\left\{\tilde{a}_i^R\tilde{a}_j^R\mathrm{tr}\left(\tilde{\boldsymbol{\Psi}}_X^{RR}\right)\right\} = \mathrm{tr}\Bigg\{\sum_l\left(\boldsymbol{A}_m\boldsymbol{G}_{\varepsilon,l}^H\otimes\boldsymbol{A}_n\boldsymbol{G}_{\varepsilon,l}^H\right) \times E^{\boldsymbol{H}}\Big\{\tilde{a}_i^R\tilde{a}_j^R\Big[\left(\Re\left(\tilde{\boldsymbol{X}}_l^H\right)\otimes\Re\left(\tilde{\boldsymbol{X}}_l^H\right)\right) \times\boldsymbol{\Omega}_{\mathrm{RR}} + \left(\Im\left(\tilde{\boldsymbol{X}}_l^H\right)\otimes\Im\left(\tilde{\boldsymbol{X}}_l^H\right)\right)\boldsymbol{\Omega}_{\mathrm{II}} - \left(\Re\left(\tilde{\boldsymbol{X}}_l^H\right)\otimes\Im\left(\tilde{\boldsymbol{X}}_l^H\right)\right)\boldsymbol{\Omega}_{\mathrm{RI}} - \left(\Im\left(\tilde{\boldsymbol{X}}_l^H\right)\otimes\Re\left(\tilde{\boldsymbol{X}}_l^H\right)\right)\boldsymbol{\Omega}_{\mathrm{IR}}\Big]\Big\}\Bigg\} \quad (50)$$

with $\boldsymbol{\Omega}_{ij}$ given by

$$\begin{aligned}\boldsymbol{\Omega}_{\mathrm{RR}} &= \Re\left(\boldsymbol{H}^H\boldsymbol{H}\right)\otimes\Re\left(\boldsymbol{H}^H\boldsymbol{H}\right)\\ \boldsymbol{\Omega}_{\mathrm{II}} &= \Im\left(\boldsymbol{H}^H\boldsymbol{H}\right)\otimes\Im\left(\boldsymbol{H}^H\boldsymbol{H}\right)\\ \boldsymbol{\Omega}_{\mathrm{RI}} &= \Re\left(\boldsymbol{H}^H\boldsymbol{H}\right)\otimes\Im\left(\boldsymbol{H}^H\boldsymbol{H}\right)\\ \boldsymbol{\Omega}_{\mathrm{IR}} &= \Im\left(\boldsymbol{H}^H\boldsymbol{H}\right)\otimes\Re\left(\boldsymbol{H}^H\boldsymbol{H}\right)\end{aligned} \quad (51)$$

We note that unlike in the case of OSTBC TED variance in [7], where we could disregard the terms involving $\boldsymbol{\Omega}_{\mathrm{RI}}$ and $\boldsymbol{\Omega}_{\mathrm{IR}}$ due to the constellation rotation, the last two terms in (50) will not average out to zero. Using the OSTBC encoding formulation of (3), we expand (50), giving (see (52))

We now consider cases where $i \neq j$ and $i = j$. Since $E\left\{\tilde{a}_i^R\tilde{a}_j^R\right\} = 0$ for $i \neq j$, in such a case only $l = 0$ with $\{k = i, k' = j\}$ and $\{k = j, k' = i\}$ terms will result in non-zero

$$E^{\boldsymbol{H}}\left\{\tilde{a}_i^R\tilde{a}_j^R\mathrm{tr}\left(\tilde{\boldsymbol{\Psi}}_X^{RR}\right)\right\} = \mathrm{tr}\Bigg\{\sum_l\left(\boldsymbol{A}_m\boldsymbol{G}_{\varepsilon,l}^H\otimes\boldsymbol{A}_n\boldsymbol{G}_{\varepsilon,l}^H\right) \times E^{\boldsymbol{H}}\Bigg\{\tilde{a}_i^R\tilde{a}_j^R\left(\sum_{k=0}^{N_s-1}\tilde{a}_{k,l}^R\boldsymbol{A}_k^H\otimes\sum_{k'=0}^{N_s-1}\tilde{a}_{k',l}^R\boldsymbol{A}_{k'}^H\right)\boldsymbol{\Omega}_{\mathrm{RR}} + \tilde{a}_i^R\tilde{a}_j^R\left(\sum_{k=0}^{N_s-1}\tilde{a}_{k,l}^I\boldsymbol{B}_k^H\otimes\sum_{k'=0}^{N_s-1}\tilde{a}_{k',l}^I\boldsymbol{B}_{k'}^H\right)\boldsymbol{\Omega}_{\mathrm{II}} + \tilde{a}_i^R\tilde{a}_j^R\left(\sum_{k=0}^{N_s-1}\tilde{a}_{k,l}^R\boldsymbol{A}_k^H\otimes\sum_{k'=0}^{N_s-1}\tilde{a}_{k',l}^I\boldsymbol{B}_{k'}^H\right)\boldsymbol{\Omega}_{\mathrm{RI}} + \tilde{a}_i^R\tilde{a}_j^R\left(\sum_{k=0}^{N_s-1}\tilde{a}_{k,l}^I\boldsymbol{B}_k^H\otimes\sum_{k'=0}^{N_s-1}\tilde{a}_{k',l}^R\boldsymbol{A}_{k'}^H\right)\boldsymbol{\Omega}_{\mathrm{IR}}\Bigg\}\Bigg\} \quad (52)$$

expectation. Thus, it can be expressed as

$$E\left\{\left(\tilde{a}_i^R\right)^2\left(\tilde{a}_j^R\right)^2\right\}\left(\boldsymbol{A}_i^H\otimes\boldsymbol{A}_j^H+\boldsymbol{A}_j^H\otimes\boldsymbol{A}_i^H\right)\boldsymbol{\Omega}_{\mathrm{RR}}$$
$$+E\left\{\tilde{a}_i^R\tilde{a}_j^R\tilde{a}_i^I\tilde{a}_j^I\right\}\left(\boldsymbol{B}_i^H\otimes\boldsymbol{B}_j^H+\boldsymbol{B}_j^H\otimes\boldsymbol{B}_i^H\right)\boldsymbol{\Omega}_{\mathrm{II}}$$
$$+E\left\{(\tilde{a}_i^R)^2\tilde{a}_j^R\tilde{a}_j^I\right\}\left(\left(\boldsymbol{A}_j^H\otimes\boldsymbol{B}_i^H\right)\boldsymbol{\Omega}_{\mathrm{RI}}+\left(\boldsymbol{B}_i^H\otimes\boldsymbol{A}_j^H\right)\boldsymbol{\Omega}_{\mathrm{IR}}\right)$$
$$+E\left\{\left(\tilde{a}_j^R\right)^2\tilde{a}_i^R\tilde{a}_i^I\right\}\left(\left(\boldsymbol{A}_i^H\otimes\boldsymbol{B}_j^H\right)\boldsymbol{\Omega}_{\mathrm{RI}}+\left(\boldsymbol{B}_j^H\otimes\boldsymbol{A}_i^H\right)\boldsymbol{\Omega}_{\mathrm{IR}}\right)\right\} \tag{53}$$

For independent and zero mean data, for which $E\{\tilde{a}_i^R\tilde{a}_i^I\}=0$ and using (13) to define ρ_2, (53) results in

$$E^{\boldsymbol{H}}\left\{\tilde{a}_i^R\tilde{a}_j^R\mathrm{tr}\left(\tilde{\boldsymbol{\Psi}}_X^{RR}\right)\right\}=\rho_2^2\mathrm{tr}\left\{\left(\boldsymbol{A}_m\boldsymbol{G}_{\varepsilon,0}^H\otimes\boldsymbol{A}_n\boldsymbol{G}_{\varepsilon,0}^H\right)\right.$$
$$\left.\times\left(\boldsymbol{A}_j^H\otimes\boldsymbol{A}_i^H+\boldsymbol{A}_i^H\otimes\boldsymbol{A}_j^H\right)\boldsymbol{\Omega}_{\mathrm{RR}}\right\}\quad i\neq j \tag{54}$$

We note that for $i\neq j$, $E\{\tilde{a}_i^R\tilde{a}_j^R\mathrm{tr}\left(\tilde{\boldsymbol{\Psi}}_X^{RR}\right)\}$ is independent of the QOSTBC rotation angle ϕ.

In the case when $i=j$ in (52), only terms for $k=k'$ will contribute to the summation. Thus, again using (3), one can express (52) for $i=j$ by

$$E^{\boldsymbol{H}}\left\{\left(\tilde{a}_i^R\right)^2\mathrm{tr}\left(\tilde{\boldsymbol{\Psi}}_X^{RR}\right)\right\}=\mathrm{tr}\left\{\sum_l\sum_{k=0}^{N_s-1}\left(\boldsymbol{A}_m\boldsymbol{G}_{\varepsilon,l}^H\otimes\boldsymbol{A}_n\boldsymbol{G}_{\varepsilon,l}^H\right)\times\right.$$
$$+E\left\{\left(\tilde{a}_i^R\right)^2\left(\tilde{a}_{k,l}^R\right)^2\right\}\left(\boldsymbol{A}_k^H\otimes\boldsymbol{A}_k^H\right)\boldsymbol{\Omega}_{\mathrm{RR}}$$
$$+E\left\{\left(\tilde{a}_i^R\right)^2\left(\tilde{a}_{k,l}^I\right)^2\right\}\left(\boldsymbol{B}_k^H\otimes\boldsymbol{B}_k^H\right)\boldsymbol{\Omega}_{\mathrm{II}}$$
$$+E\left\{\left(\tilde{a}_i^R\right)^2\left(\tilde{a}_{k,l}^R\right)\left(\tilde{a}_{k,l}^I\right)\right\}$$
$$\left.\times\left(\left(\boldsymbol{A}_k^H\otimes\boldsymbol{B}_k^H\right)\boldsymbol{\Omega}_{\mathrm{RI}}+\left(\boldsymbol{B}_k^H\otimes\boldsymbol{A}_k^H\right)\boldsymbol{\Omega}_{\mathrm{IR}}\right)\right\} \tag{55}$$

We first consider the case where $l\neq 0$ or $l=0$, $k\neq i$. Referring to the three summation terms in (55), we note that

$$E\left\{\left(\tilde{a}_i^R\right)^2\left(\tilde{a}_{k,l}^R\right)^2\right\}=\rho_{2\phi}^2=\rho_2^2\quad l\neq 0,\{l=0,k\neq i\}$$
$$E\left\{\left(\tilde{a}_i^R\right)^2\left(\tilde{a}_{k,l}^I\right)^2\right\}=\rho_{2\phi}^2=\rho_2^2\quad l\neq 0,\{l=0,k\neq i\} \tag{56}$$
$$E\left\{\left(\tilde{a}_i^R\right)^2\tilde{a}_{k,l}^R\tilde{a}_{k,l}^I\right\}=0\quad l\neq 0,\{l=0,k\neq i\}$$

where we have defined

$$\rho_{2\phi}\triangleq E\left\{\left(\tilde{a}_i^R\right)^2\right\} \tag{57}$$

The equivalence of $\rho_{2\phi}$ and ρ_2 can easily be shown using (2) [11]. For $l=0$ and $k=i$, we have

$$E\left\{\left(\tilde{a}_i^R\right)^2\left(\tilde{a}_{k,l}^R\right)^2\right\}=E\left\{\left(\tilde{a}_i^R\right)^4\right\}\triangleq\rho_{4\phi}$$
$$E\left\{\left(\tilde{a}_i^R\right)^2\left(\tilde{a}_{k,l}^I\right)^2\right\}=E\left\{\left(\tilde{a}_i^R\right)^2\left(\tilde{a}_i^I\right)^2\right\}\triangleq\rho_{2\phi}' \tag{58}$$
$$E\left\{\left(\tilde{a}_i^R\right)^2\left(\tilde{a}_{k,l}^R\right)\left(\tilde{a}_{k,l}^I\right)\right\}=E\left\{\left(\tilde{a}_i^R\right)^3\tilde{a}_i^I\right\}\triangleq\rho_{\phi}''$$

The constants $\rho_{4\phi}$, $\rho_{2\phi}'$ and ρ_{ϕ}'' have been evaluated for M-PSK constellations in [11]. After some algebraic manipulation, (55) can be expressed as (see (59))

Having considered the data component of (46), we now focus on the noise term involving $\tilde{\boldsymbol{\Psi}}_N^{RR}$, that is

$$E^{\boldsymbol{H}}\left\{\tilde{a}_i^R\tilde{a}_j^R\mathrm{tr}\left(\tilde{\boldsymbol{\Psi}}_N^{RR}\right)\right\}=$$
$$E^{\boldsymbol{H}}\left\{\tilde{a}_i^R\tilde{a}_j^R\mathrm{tr}\left\{\boldsymbol{A}_m\Re\left(\boldsymbol{N}^H\boldsymbol{H}\right)\otimes\boldsymbol{A}_n\Re\left(\boldsymbol{N}^H\boldsymbol{H}\right)\right\}\right\} \tag{60}$$

We note that, since $E\{\tilde{a}_i^R\tilde{a}_j^R\}=0$ for $i\neq j$, we need to consider only the case for $i=j$. Furthermore, since $E\{\left(\tilde{a}_i^R\right)^2\}=E\{\left(a_i^R\right)^2\}=\rho_2$, (60) will result in the same solution as for the OSTBC derived in [7], that is

$$E^{\boldsymbol{H}}\left\{\left(\tilde{a}_i^R\right)^2\mathrm{tr}\left(\tilde{\boldsymbol{\Psi}}_N^{RR}\right)\right\}=$$
$$\rho_2\frac{N_0}{2}\mathrm{tr}\left\{\left(\boldsymbol{A}_m\otimes\boldsymbol{A}_n\right)\boldsymbol{\Lambda}_N\left(\boldsymbol{\Omega}'_{\mathrm{RR}}+\boldsymbol{\Omega}'_{\mathrm{II}}\right)\right\} \tag{61}$$

$$E^{\boldsymbol{H}}\left\{\left(\tilde{a}_i^R\right)^2\mathrm{tr}\left(\tilde{\boldsymbol{\Psi}}_X^{RR}\right)\right\}=\rho_2^2\mathrm{tr}\left\{\sum_l\sum_k\left(\boldsymbol{A}_m\boldsymbol{G}_{\varepsilon,l}^H\otimes\boldsymbol{A}_n\boldsymbol{G}_{\varepsilon,l}^H\right)\right.$$
$$\left.\times\left[\left(\boldsymbol{A}_k^H\otimes\boldsymbol{A}_k^H\right)\boldsymbol{\Omega}_{\mathrm{RR}}+\left(\boldsymbol{B}_k^H\otimes\boldsymbol{B}_k^H\right)\boldsymbol{\Omega}_{\mathrm{II}}\right]\right\}$$
$$+\mathrm{tr}\left\{\left(\boldsymbol{A}_m\boldsymbol{G}_{\varepsilon,0}^H\otimes\boldsymbol{A}_n\boldsymbol{G}_{\varepsilon,0}^H\right)\right.$$
$$\times\left[\left(\rho_{4\phi}-\rho_2^2\right)\left(\boldsymbol{A}_i^H\otimes\boldsymbol{A}_i^H\right)\boldsymbol{\Omega}_{\mathrm{RR}}\right.$$
$$+\left(\rho_{2\phi}'-\rho_2^2\right)\left(\boldsymbol{B}_i^H\otimes\boldsymbol{B}_i^H\right)\boldsymbol{\Omega}_{\mathrm{II}}$$
$$\left.\left.+\rho_{\phi}''\left(\left(\boldsymbol{A}_i^H\otimes\boldsymbol{B}_i^H\right)\boldsymbol{\Omega}_{\mathrm{RI}}+\left(\boldsymbol{B}_i^H\otimes\boldsymbol{A}_i^H\right)\boldsymbol{\Omega}_{\mathrm{IR}}\right)\right]\right\} \tag{59}$$

doi: 10.1049/iet-com.2012.0244

where $\mathbf{\Lambda}_N$ is defined by

$$\mathbf{\Lambda}_N(i,j) = \begin{cases} 1, & i = nN_r + n + 1, j = mN_c + m + 1 \\ 0, & \text{elsewhere} \end{cases} \quad (62)$$

for $n = 0, \ldots, N_r - 1$ and $m = 0, \ldots, N_c - 1$. In (61) $\boldsymbol{\Omega}'_{ij}$ are given by

$$\begin{aligned} \boldsymbol{\Omega}'_{\mathrm{RR}} &= \Re(\boldsymbol{H}) \otimes \Re(\boldsymbol{H}) \\ \boldsymbol{\Omega}'_{\mathrm{II}} &= \Im(\boldsymbol{H}) \otimes \Im(\boldsymbol{H}) \\ \boldsymbol{\Omega}'_{\mathrm{RI}} &= \Re(\boldsymbol{H}) \otimes \Im(\boldsymbol{H}) \\ \boldsymbol{\Omega}'_{\mathrm{IR}} &= \Im(\boldsymbol{H}) \otimes \Re(\boldsymbol{H}) \end{aligned} \quad (63)$$

Finally, combining (54), (59) and (61) with (46), we obtain the solution to $E^{\boldsymbol{H}}\left\{\tilde{a}_i^R \tilde{a}_j^R \tilde{\zeta}_m^R \tilde{\zeta}_n^R\right\}$, given by

$$E^{\boldsymbol{H}}\left\{\tilde{a}_i^R \tilde{a}_j^R \tilde{\zeta}_m^R \tilde{\zeta}_n^R\right\} = \|\boldsymbol{H}\|^{-4}\mathrm{tr}\left\{\rho_2^2 \tilde{\boldsymbol{\Phi}}_{ijmn}^{RR} + \rho_2 \frac{N_0}{2} \tilde{\boldsymbol{\Delta}}_{ijmn}^{RR}\right\} \quad (64)$$

where $\tilde{\boldsymbol{\Phi}}_{ijmn}^{RR}$ and $\tilde{\boldsymbol{\Delta}}_{ijmn}^{RR}$ are given by (25) and (26), respectively.